Наносистеми, наноматеріали, нанотехнології
Nanosistemi, Nanomateriali, Nanotehnologii
2019, т. 17, № 3, сс. 557–566

PACS numbers: 05.10.Ln, 05.70.Ce, 64.75.Ef, 65.40.gd, 81.30.Bx, 81.30.Fb, 82.60.Lf

Modelling of Transition Metal High-Entropy Solid Solutions

A. B. Melnick[1], V. Ya. Beloshapka[2], and V. K. Soolshenko[1]

[1]*G. V. Kurdyumov Institute for Metal Physics, N.A.S. of Ukraine,*
36, Academician Vernadsky Blvd.,
UA-03142 Kyiv, Ukraine
[2]*Berdyansk State Pedagogical University,*
4, Schmidt Str.,
UA-71100 Berdyansk, Ukraine

The compositions of high-entropy alloys based on the elements Ni, Co, Fe, Cr, Mn, Ti, V, Cu, Al, Zr, and Si are evaluated with use of thermodynamic approach. Optimal compositions for alloys with minimal Gibbs energy are obtained, and influence of various factors on formation of the alloys is described. As shown, the most stable alloys are nonequiatomic. The compositions for alloys, which will be in the state of homogeneous multicomponent solid solutions, are determined.

Композиції для високоентропійних стопів на основі елементів Ni, Co, Fe, Cr, Mn, Ti, V, Cu, Al, Zr, Si оцінювали з використанням термодинамічного підходу. Одержано оптимальні концентрації для стопів з мінімальною Ґіббсовою енергією та описано вплив різних чинників на їх формування. Показано, що найстабільніші стопи не є еквіатомовими. Визначено склади стопів, які перебуватимуть у стані однорідних багатокомпонентних твердих розчинів.

Составы высокоэнтропийных сплавов на основе элементов Ni, Co, Fe, Cr, Mn, Ti, V, Cu, Al, Zr, Si рассматривались с использованием термодинамического подхода. Получены оптимальные концентрации для сплавов с минимальной энергией Гиббса и описано влияние различных факторов на их формирование. Было показано, что наиболее стабильные сплавы не являются эквиатомными. Определены составы сплавов, которые будут находиться в состоянии однородных многокомпонентных твёрдых растворов.

Key words: high-entropy alloys, solid solution, Gibbs energy, transition metals.

Ключові слова: високоентропійні стопи, твердий розчин, Ґіббсова енер-

гія, перехідні метали.

Ключевые слова: высокоэнтропийные сплавы, твёрдый раствор, энергия Гиббса, переходные металлы.

(Received 27 March, 2019)

1. INTRODUCTION

The idea of high-entropy alloys (HEAs) was proposed by Yeh *et al.* in 2004 [1] and based on the concept that the high configurational entropy would stabilize the solid solution (SS) phase. HEAs are multicomponent (5 or more) bulk solid solutions, intermetallics or glasses with near equiatomic composition [1–5]. This can provide a large value of change mixing entropy (ΔS_{mix}) for the formation of homogeneous system. For regular solution,

$$\Delta S_{\text{mix}} = -k\sum_{i=1}^{n} c_i \ln\left(c_i\right), \tag{1}$$

where c_i is the atomic fraction of i-th element, k—Boltzmann constant.

According to (1), the maximum effect of the entropy factor will be for the equiatomic case.

In recent years, high-entropy solid solutions (HESS) have attracted increasing attentions, because they exhibit special structure and unique properties. Many HEA studies are devoted to the search for single-phase SS [6, 7].

The thermodynamic properties of alloy are very important for understanding of relative stability of single-phase SS. In concordance with thermodynamics, a system will be in a stable equilibrium state, if it has the lowest Gibbs free energy. The difference between the Gibbs free energy of solid phase and liquid state is as follows:

$$\Delta G = \Delta H - T\Delta S,$$

where ΔH is the formation enthalpy, T—absolute temperature, S—total entropy.

Many methods have been devised to estimate the formation enthalpies and other thermodynamic properties of alloys with a single solid-solution phase:

1) first-principles' calculations within the framework of density functional theory combined with atomistic simulation techniques like *ab initio* calculations, molecular dynamics simulations, and Monte Carlo methods [8–13];
2) solution thermodynamics based on extrapolation of experimental

data as in the CALPHAD [14–16];

3) semi-empirical Miedema's model and empirical thermophysical parameters based on the Hume-Rothery rules [17].

It should be noted that first-principle calculations and atomistic simulation techniques have a high computational difficulties for multicomponent systems. The CALPHAD method needs extensive database of experimental thermodynamic functions of multicomponent alloys. Various thermophysical parameters were proposed to predict formation of single-phase solid solutions. Among them are: mixing entropy ΔS_{mix} [18], mixing enthalpy ΔH_{mix} [18], differences of atomic sizes δ_r [18], $\Omega = T_m \Delta S_{\text{mix}} / |\Delta H_{\text{mix}}|$ [19], valence-electron concentration (VEC) [20], electronegativity difference δ_χ [21], the φ-parameter [22] and other. An analysis of these parameters gives possibility to conclude, whether the alloy will be in the state of solid solution. However, such an approach is semi-quantitative and do not allow to optimize the alloy composition. For estimations that are more accurate, the Miedema's method has to be adapted. Takeuchi and Inoue [23] supposed that, for multicomponent glasses, ΔG is proportional to free energy ΔG_{mix} of liquid-phases' mixing:

$$\Delta G_{\text{mix}} = \Delta H_{\text{mix}} - T \Delta S_{\text{mix}};$$

here, H_{mix} is an enthalpy of mixing. In solid solutions, where atoms of different sizes occupy equivalent lattice positions, an additional elastic contribution (ΔH_{el}) has to be taken into account:

$$\Delta H = \Delta H_{\text{mix}} + \Delta H_{\text{el}}, \;\; \Delta G = \Delta H_{\text{mix}} + \Delta H_{\text{el}} - T \Delta S_{\text{mix}} . \qquad (2)$$

Regular solution model has been adopted in order to simplify the calculation of (2) and for minimization of ΔG on element concentrations [24]. Thus, it is possible to obtain the most stable multicomponent solutions.

Since Cantor alloy [25], single-phase NiCoFeCr-based HEAs are the promising materials with high tensile ductility and fracture toughness [26]. Development of NiCoFeCr-based HEAs was continued by adding elements into equiatomic NiCoFeCr base for strengthening. The composition of the most stable HEA may be different from the equiatomic one because some contributions additional to entropy. To find the compositions of stable solid solutions including Ni, Co, Fe, Cr, Mn, Ti, V, Cu, Al, Zr, Si elements, we minimize Gibbs free energies of investigated systems.

2. MODELLING

Compositions for HEAs with minimal Gibbs free energy were ob-

tained based on thermodynamic approach developed in the article [24], where substitutional solid solutions were considered with the regular-solution approximation. The parameters for expression (2) were determined as follow. The mixing enthalpy of multicomponent alloy consisting of n elements is as follows [27]:

$$\Delta H_{\text{mix}} = \sum_{i,j=1 \quad i \neq j}^{n} c_i c_j \Omega_{ij} , \tag{3}$$

where Ω_{ij} is parameter characterizing the interaction between i-th and j-th elements of the regular solution; $\Omega_{ij} = 4\Delta H^{ij}_{\text{mix}}$; c_i—atomic fraction of i-th component; $\Delta H^{ij}_{\text{mix}}$—mixing enthalpy for binary liquid equiatomic alloy. The values $\Delta H^{ij}_{\text{mix}}$ were taken from Ref. [28].

The elastic distortion energy for the solid solution ΔH_{el} is:

$$\Delta H_{\text{el}} = \sum_{i=1}^{n} c_i B_i \frac{\left(V_i(T) - V(T)\right)^2}{2V_i(T)} ; \tag{4}$$

here, $V(T)$ is the average volume of atom in the alloy; $V_i(T)$—atomic volume and B_i—bulk modulus of i-th element.

$$V_i(T) = V_{0i}\left(1 + \alpha_i \left(T - T_0\right)\right)^3 ,$$

α_i is linear expansion coefficient for the i-th component; $T_0 = 293$ K.

$$V(T) = \sum_{i=1}^{n} c_i B_i V_i(T) \Big/ \sum_{i=1}^{n} c_i B_i .$$

The effective melting temperature of solid solution, T_m, was calculated as

$$T_m = \sum_{i=1}^{n} c_i T_m^i ,$$

where T_m^i is melting temperature of the i-th element.

Then, Gibbs free-energy concentration dependence can be written as

$$\Delta G\left(c_i\right)_{i=1 \div n} = \sum_{i,j=1 \quad i \neq j}^{n} c_i c_j \Omega_{ij} + \sum_{i=1}^{n} c_i B_i \frac{\left(V_i(T) - V(T)\right)^2}{2V_i(T)} - kT_m \sum_{i=1}^{n} c_i \ln(c_i) . \tag{5}$$

ΔG minimization was carried out using the Monte Carlo method. The values of the constants α_i, V_{0i}, B_i, T_m^i in expression (5) were taken from tables of Ref. [29]. The minima of ΔG correspond to the compositions of stable alloys. To analyse the state of alloys, a number parameters were used: ΔG, ΔH_{mix}, ΔH_{el}, ΔS_{mix}, T_m, and

$$\Omega = T_m \Delta S_{\text{mix}} / |\Delta H_{\text{mix}}|,$$

$$\delta = \sqrt{\sum_{i=1}^{n} c_i \left(1 - \frac{r_i}{\bar{r}}\right)^2},$$

where $r_i = \left(V_{0i}\right)^{1/3}$, $\bar{r} = \sum_{i=1}^{n} c_i r_i$.

3. RESULTS AND DISCUSSION

The calculation results are summarized in tables for different element combinations (Table 1 for equiatomic alloys and Table 2 for alloys with minimal Gibbs free energy).

TABLE 1. Calculated parameters ΔG, ΔH_{mix}, ΔH_{el}, δ, Ω, ΔS_{mix}, and T_m for equiatomic alloys.

No.	Alloys	ΔG, kJ/mol	ΔH_{mix}, kJ/mol	ΔH_{el}, kJ/mol	δ, %	Ω	ΔS_{mix}, J/(mol·K)	T_m, K
1	NiCoFe	–16.971	–1.333	0.5221	1.068	12.119	9.135	1769
2	NiCoCr	–21.873	–4.889	0.2988	1.373	3.535	9.135	1892
3	CoFeCr	–19.853	–2.667	0.3492	1.134	6.576	9.135	1920
4	NiCoFeCr	–24.850	–3.750	0.4755	1.306	5.753	11.527	1872
5	NiCoFeCrCu	–19.784	3.200	0.6889	1.241	7.398	13.382	1769
6	NiCoFeCrAl	–24.896	–12.320	9.959	5.281	1.829	13.382	1684
7	NiCoFeCrSi	–31.258	–26.400	19.695	7.966	0.930	13.382	1834
8	NiCoFeCrMn	–26.864	–4.160	1.400	1.454	5.7941	13.382	1801
9	NiCoFeCrTi	–27.569	–16.320	13.984	6.153	1.5461	13.382	1886
10	NiCoFeCrZr	–23.063	–22.720	25.390	10.21	1.132	13.382	1923
11	NiCoFeCrV	–31.089	–8.960	3.752	2.896	2.888	13.382	1934
12	NiCoFeCrCuAl	–20.823	–4.778	8.233	4.867	5.081	14.898	1630
13	NiCoFeCrCuAlSi	–25.463	–18.857	19.894	7.476	1.405	16.180	1638
14	NiCoFeCrCuAlSiV	–31.985	–20.687	18.199	7.00	1.425	17.290	1706
15	NiCoFeCrCuAlMnV	–28.919	–7.625	7.840	4.424	3.821	17.290	1685
16	NiCoFeCrCuMnV	–27.841	–1.959	3.119	2.467	14.802	16.180	1792
17	NiCoFeCrCuAlM*n*TiZrV	–30.050	–18.840	22.387	8.186	1.783	19.145	1755

TABLE 2. Calculated parameters ΔG, ΔH_{mix}, ΔH_{el}, δ, Ω, ΔS_{mix}, and T_m for alloys with minimal Gibbs free energy.

No.	Alloys	ΔG, kJ/mol	ΔH_{mix}, kJ/mol	ΔH_{el}, kJ/mol	δ, %	Ω	ΔS_{mix}, J/(mol·K)	T_m, K
1	$Ni_{33}\,Co_{31.2}\,Fe_{35.8}$	–16.995	–1.392	0.543	1.088	11.60	9.121	1770
2	$Ni_{32.3}\,Co_{24.2}Cr_{43.5}$	–22.506	–5.618	3.288	1.451	3.064	8.901	1934
3	$Co_{33.4}\,Fe_{26.1}\,Cr_{40.5}$	–20.136	–2.936	3.231	1.165	5.968	9.004	1946
4	$Ni_{26.2}Co_{20.1}Fe_{17.4}Cr_{36.3}$	–25.574	–4.588	4.335	1.368	4.669	11.188	1915
5	$Ni_{26}Co_{19.9}Fe_{17.2}Cr_{35.9}Cu_1$	–25.729	–4.147	4.491	1.364	5.312	11.542	1909
6	$Ni_{25.6}Co_{19.2}Fe_{15.5}Cr_{32.2}Al_{7.5}$	–27.029	–8.195	4.256	3.667	2.818	12.587	1834
7	$Ni_{20.3}Co_{15.6}Fe_{15.2}Cr_{31.5}Si_{17.4}$	–32.089	–24.702	17.151	7.515	0.993	13.038	1882
8	$Ni_{24.8}Co_{18.4}Fe_{14.9}Cr_{29.8}Mn_{12.1}$	–27.615	–4.646	1.0782	1.456	5.175	12.948	1857
9	$Ni_{28.5}Co_{19.5}Fe_{14.9}Cr_{23.2}Ti_{13.9}$	–28.414	–14.062	10.278	5.471	1.751	13.083	1883
10	$Ni_{28.6}Co_{20.7}Fe_{15.8}Cr_{28.4}Zr_{6.5}$	–26.896	–11.650	8.668	6.616	2.052	12.561	1904
11	$Ni_{24.1}Co_{17}Fe_{12.6}Cr_{18}V_{28.3}$	–31.763	–11.134	4.913	3.255	2.294	13.063	1955
12	$Ni_{25.4}Co_{19.1}Fe_{15.3}Cr_{32.1}Cu_{0.8}Al_{7.2}$	–27.149	–7.754	4.160	3.625	3.037	12.854	1832
13	$Ni_{20}Co_{15.2}Fe_{14.5}Cr_{30.4}Cu_{0.5}Al_{2.8}Si_{16.6}$	–32.647	–24.531	17.685	7.50	1.052	13.927	1853
14	$Ni_{1.5}Co_{1.1}Fe_{1.7}Cr_{1.3}Cu_{0.1}Al_{5.6}Si_{38.5}V_{50.2}$	–44.045-	–45.133-	18.81515	6.326	0.393	9.313	1903
15	$Ni_{21.3}Co_{14.5}Fe_{9.8}Cr_{13.2}Cu_{0.6}Al_7Mn_{7.7}V_{25.9}$	–34.412	–13.353	7.611	4.161	2.147	15.535	1845
16	$Ni_{22.8}Co_{15.7}Fe_{11.3}Cr_{16.1}Cu_{0.7}Mn_{7.4}V_{26}$	–33.133	–10.05631	4.745	3.134	2.7673	14.516	1917
17	$Ni_{22.2}Co_{14}Fe_{8.6}Cr_{10.2}Cu_{0.6}Al_{7.3}Mn_{6.6}Ti_{7.2}\ Ti_4\ Zr_{1.9}V_{21.4}$	–36.052	–18.38708	13.566	6.024	1.698	17.0372	1833

Optimized alloy compositions differ significantly from equiatomic. Gibbs free-energy–composition diagrams for ternary and quasi-ternary alloy systems (Figs. 1, 2) illustrate the differences of compositions.

If we consider a system consisting of 4 base elements (Ni, Co, Fe, Cr), we can observe the existence of a wide range of concentrations near the equiatomic point, where a single solid solution will be formed (see Fig. 1 and Tables 1, 2). CALPHAD calculations with experimental verifications [26] indicate the same result.

What elements can be added to the base composition to reduce Gibbs energy and not destroy the solid solution? Let us explore this question. If we examine equiatomic compositions (see Table 1), the additions of Al, Si, Mn, Ti, V to the base elements decreases the Gibbs energy, while other components increase it more (Cu) or less (Zr). Parameters ΔH_{mix}, δ, Ω play a special role in formation of solid solutions. When $\delta < 6\%$ and $\Delta H_{\text{mix}} > -10$ kJ/mol, solid solution is

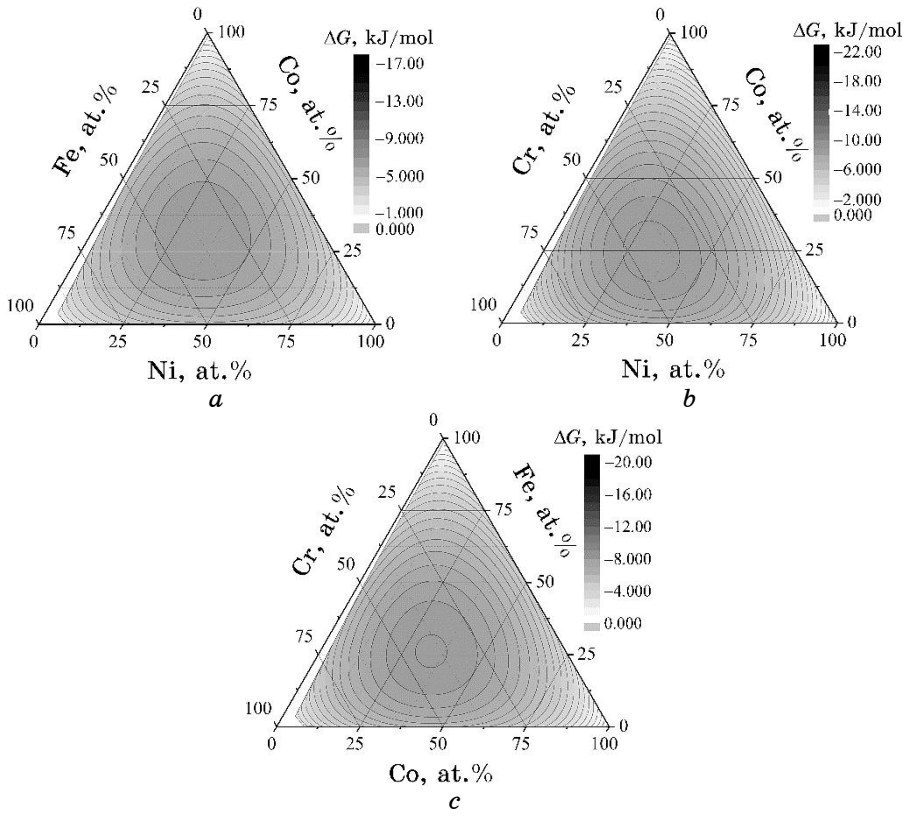

Fig. 1. The calculated Gibbs free energy of solid solutions (ΔG) for ternary Ni–Co–Fe (*a*), Ni–Co–Cr (*b*), Co–Fe–Cr (*c*) alloy systems.

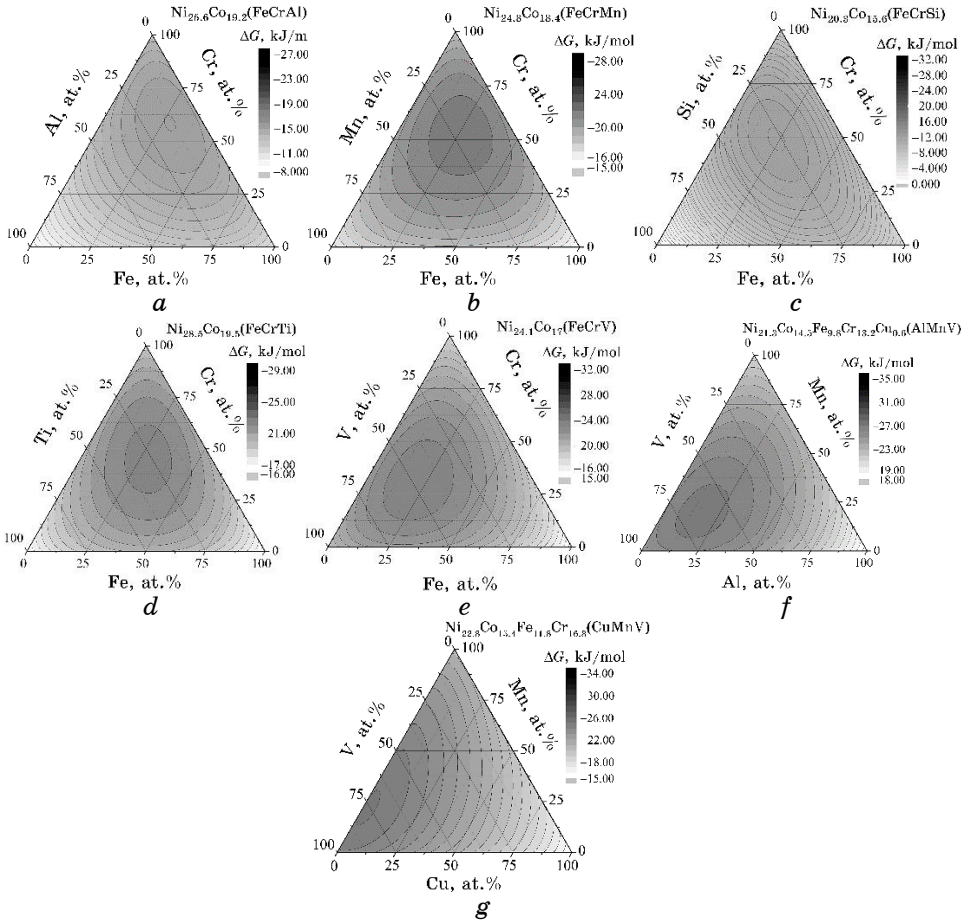

Fig. 2. The calculated Gibbs free energy of solid solutions (ΔG) for quasi-ternary $Ni_{25.6}Co_{19.2}$(FeCrAl) (*a*), $Ni_{24.8}Co_{18.4}$(FeCrMn) (*b*), $Ni_{20.3}Co_{15.6}$(FeCrSi) (*c*), $Ni_{28.5}Co_{19.5}$(FeCrTi) (*d*), $Ni_{24.1}Co_{17}$(FeCrV) (*e*), $Ni_{21.3}Co_{14.5}Fe_{9.8}Cr_{13.2}Cu_{0.6}$ (AlMnV) (*f*), $Ni_{22.8}Co_{15.4}Fe_{11.8}Cr_{16.8}$ (CuMnV) (*g*) alloy systems.

crystallized [30].

According to Ref. [31], relations $\Omega \geq 1.1$ and $\delta \leq 6.6\%$ should be considered as criteria for forming solid-solution phase. Thus, it can be concluded that the (NiCoFeCr, NiCoFeCrCu, NiCoFeCrAl, NiCoFeCrMn, NiCoFeCrV, NiCoFeCrCuAl, NiCoFeCrCuMnV, NiCoFeCrCuAlMnV) equiatomic alloys will crystallize as a solid solution. Addition of silicon to the base elements leads to a significant decrease in Gibbs energy, but, at the same time, the energy of elastic deformation increases to a level incompatible with the existence of a solid solution.

Using optimization procedure, we obtain alloys, which are superi-

or in energy stability as compared to equiatomic ones (Table 2). They differ in composition from equiatomic HEAs. Let us consider these differences. If we consider the relationship between the base components (Ni, Co, Fe, Cr) in optimized alloys, the element predominance (Cr in system 2, 3, 4, 5, 6, 7, 8, 12, 13 of Table 2; Ni in system 9, 10, 11, 15, 16, 17 of Table 2) is observed. Optimization of compositions leads to a significant decrease in Gibbs energy mainly due to a change in the energy of elastic distortions, enthalpy of mixing, or melting temperature.

4. CONCLUSIONS

1. Compositions of alloys based on Ni, Co, Fe, Cr, Mn, Ti, V, Cu, Al, Zr, Si elements with minimal Gibbs free energy were calculated using thermodynamic approach in approximation of regular solid-solution model.
2. The alloy compositions with minimal Gibbs free energy differ considerably from equiatomic ones.
3. The compositions of alloys favourable for formation of single-phase solid solutions were determined.

REFERENCES

1. J. W. Yeh, S. K. Chen, S. J. Lin, J. Y. Gan, T. S. Chin, T. T. Shun et al., *Adv. Eng. Mater.*, **6**: 299 (2004); https://doi.org/10.1002/adem.200300567.
2. J. W. Yeh, *JOM*, **65**: 1759 (2013); https://doi.org/10.1007/s11837-013-0761-6.
3. Y. Zhang, T.T. Zuo, Z. Tang et al., *Progress in Materials Science*, **61**: 1 (2014); https://doi.org/10.1016/j.pmatsci.2013.10.001.
4. M. H Tsai and J. W. Yeh, *Mater. Res. Lett.*, **2**: 107 (2014); https://doi.org/10.1080/21663831.2014.912690.
5. D. B. Miracle and O. N. Senkov, *Acta Mater.*, **122**: 448 (2017); https://doi.org/10.1016/j.actamat.2016.08.081.
6. M. C. Gao, C. Zhang, P. Gao, F. Zhang, L. Z. Ouyang, M. Widom, and J. A. Hawk, *Curr. Opin. Solid State Mater. Sci.*, **21**: 238 (2017); https://doi.org/10.1016/j.cossms.2017.08.001.
7. Y. Tan, J. Li, S. Tang, J. Wang, and H. Kou, *Journal of Alloys and Compounds*, **742**: 430 (2018); https://doi.org/10.1016/j.jallcom.2018.01.252.
8. F. Tian, L. K. Varga, N. Chen, L. Delczeg, and L. Vitos, *Phys. Rev. B*, **87**: 075144 (2013); https://doi.org/10.1103/PhysRevB.87.075144.
9. F. Tian, L. Delczeg, N. Chen, L. K. Varga, J. Shen, and L. Vitos, *Phys. Rev. B*, **88**: 085128 (2013); https://doi.org/10.1103/PhysRevB.88.085128.
10. P. Singh, A. V. Smirnov, and D. D. Johnson, *Phys. Rev. B*, **91**: 224204 (2015); https://doi.org/10.1103/PhysRevB.91.224204.
11. D. Ma, B. Grabowski, F. Körmann, J. Neugebauer, and D. Raabe, *Acta Mater.*, **100**: 90 (2015); https://doi.org/10.1016/j.actamat.2015.08.050.
12. C. Jiang and B. P. Uberuaga, *Phys. Rev. Lett.*, **116**: 105501 (2016);

https://doi.org/10.1103/PhysRevLett.116.105501.
13. M. C. Troparevsky, J. R. Morris, P. R. C. Kent, A. R. Lupini, G. M. Stocks, *Phys. Rev. X*, **5**: 011041 (2015); https://doi.org/10.1103/PhysRevX.5.011041.
14. F. Zhang, C. Zhang, S. L. Chen, J. Zhu, W. S. Cao, and U. R. Kattner, *CALPHAD*, **5**: 1 (2014); https://doi.org/10.1016/j.calphad.2013.10.006.
15. C. Zhang, F. Zhang, S. Chen, and W. Cao, *JOM*, **64**: 839 (2012); https://doi.org/10.1007/s11837-012-0365-6.
16. O. N. Senkov, J. D. Miller, D. B. Miracle, and C. Woodward, *Nature Comm.*, **6**: 6529 (2015); https://doi.org/10.1038/ncomms7529.
17. U. Mizutani, *Hume-Rothery Rules for Structurally Complex Alloy Phases* (Boca Raton: CRC Press: 2010).
18. Y. Zhang, Y. J. Zhou, J. P. Lin, G. L. Chen, P. K. Liaw, *Adv. Eng. Mater.*, **10**: 534 (2008); https://doi.org/10.1002/adem.200700240.
19. Y. Zhang, Z. P. Lu, S. G. Ma, P. K. Liaw, Z. Tang, Y. Q. Cheng et al., *MRS Commun.*, **4**: 57 (2014); https://doi.org/10.1557/mrc.2014.11.
20. S. Guo, C. Ng, J. Lu, and C. T. Liu, *J. Appl. Phys.*, **109**: 103505 (2011); https://doi.org/10.1063/1.3587228.
21. S. Fang, X. Xiao, L. Xia, W. Li, and Y. Dong, *J. Non-Cryst. Solids*, **321**: 120 (2003); https://doi.org/10.1016/S0022-3093(03)00155-8.
22. Y. F. Ye, Q. Wang, J. Lu, C. T. Liu, and Y. Yang, *Scripta Mater.*, **104**: 53 (2015); https://doi.org/10.1016/j.scriptamat.2015.03.023.
23. A. Takeuchi and A. Inoue, *Sci. Eng. A*, **304–306**: 446 (2001); https://doi.org/10.1016/S0921-5093(00)01446-5.
24. A. B. Melnick and V. K. Soolshenko, *Journal of Alloys and Compounds*, **694**: 223 (2017). https://doi.org/10.1016/j.jallcom.2016.09.189
25. B. Cantor, I. Chang, P. Knight, and A. Vincent, *Mater. Sci. Eng. A*, **375–377**: 213 (2004); https://doi.org/10.1016/j.msea.2003.10.257.
26. F. He, Z. Wang, Q. Wu, S. Niu, J. Li, J. Wang, and C. T. Liu, *Scripta Materialia*, **131**: 42 (2017); https://doi.org/10.1016/j.scriptamat.2016.12.033.
27. A. Takeuchi and A. Inoue, *Materials Transactions*, **41**: 1372 (2000); https://doi.org/10.2320/matertrans1989.41.1372.
28. A. Takeuchi and A. Inoue, *Materials Transactions*, **46**: 2817 (2005); https://doi.org/10.2320/matertrans.46.2817.
29. *WebElements Periodic Table*, http://www.webelements.com/.
30. Y. Zhang, Y. J. Zhou, J. P. Lin, G. L. Chen, and P. K. Liaw, *Adv. Eng. Mater.*, **10**: 534 (2008); https://doi.org/10.1002/adem.200700240.
31. X. Yang and Y. Zhang, *Mater. Chem. Phys.*, **132**: 233 (2012); https://doi.org/10.1016/j.matchemphys.2011.11.021.